Thermal Simulation of Electric Vehicle Battery

Shaurya Sarna

IIT Bombay

Abstract

This project deals with thermal modeling of a segment comprising Li-ion cells. With the given conditions of airflow rate and heat flux, the source's temperature (cell connections) is observed over the entire duration of the simulation. The results show the maximum temperature attained by the region in scrutiny and helps to validate the real-time performance.

1. Introduction

Electric vehicles (EVs) can be considered one of the most promising technologies to counter environmental problems. The whole concept of EVs majorly boils down to its two components, motors, and batteries. Batteries act as the powerhouse to propel the vehicle. With the new age lithium-ion cells, certain restrictions come up. These cells need very precise temperature conditions to give the best performance and extend the life. Thus, thermal analysis of batteries becomes an essential step while designing EVs.

Various cooling methods are being used to cool down the cells. These include, but not limited to, forced convection using air, liquid immersion cooling, microfluidic channels, conduction using heat sinks, and phase change materials. All these have their advantages and limitations. Air cooling is the simplest to implement and safest of all. However, it is the most bulkiest of the above-listed methods.

2. Problem Statement

The objective is to observe the variation of temperature close to the heat source over a fixed interval of time. The heat sources are regions where terminals of two cells come in contact and generate heat due to contact resistance. Forced convection is used to cool these regions with the help of air.

3. Governing Equations

Following sets of equations are solved using BuoyantPimpleFoam:

Mass Conservation:

$$\frac{\partial \rho}{\partial t} + \nabla.(\rho \boldsymbol{u}) = 0 \quad (1)$$

Momentum Conservation

$$\frac{\partial(\rho \boldsymbol{u})}{\partial t} + \nabla.(\rho \boldsymbol{u}\boldsymbol{u}) = -\nabla p + \rho \boldsymbol{g} + \nabla.\left(2\mu_{eff} D(\boldsymbol{u})\right) - \nabla(\frac{2}{3}\mu_{eff}(\nabla.\boldsymbol{u})) \quad (2)$$

Energy Conservation (sensibleInternalEnergy)

$$\frac{\partial(\rho e)}{\partial t} + \nabla.(\rho \boldsymbol{u} e) + \frac{\partial(\rho K)}{\partial t} + \nabla.(\rho \boldsymbol{u} K) + \nabla.(\rho \boldsymbol{u}) = \nabla.\left(\alpha_{eff} \nabla e\right) + \rho \boldsymbol{u}.\boldsymbol{g} \quad (3)$$

Two basic heat transfer equations (forced convection) are focused on in this problem:

$$mC_P \frac{dT}{dt} = I^2 R - Q_{conv} \quad (4)$$

$$Q_{conv} = hA(T - T_S) \quad (5)$$

Where

mC_P = Cell tab properties

I = Current through cell

R = Contact resistance between cell tabs

Q_{conv} = Heat transfer due to forced convection

H = Convective heat transfer coefficient

A = Cell tab surface area

T = Cell tab temperature

T_S = Inlet air temperature

4. Simulation Procedure

4.1 Geometry and Mesh

The geometry is a simple cuboidal box, with two air inlet slits on top, two heat sources on the bottom, and one outlet face. The geometry is shown in the following figures:

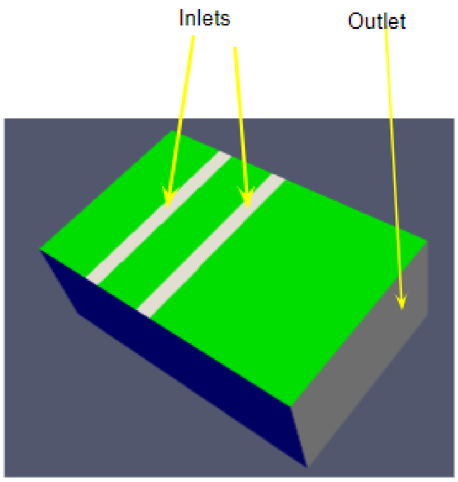

Figure 1 - Geometry

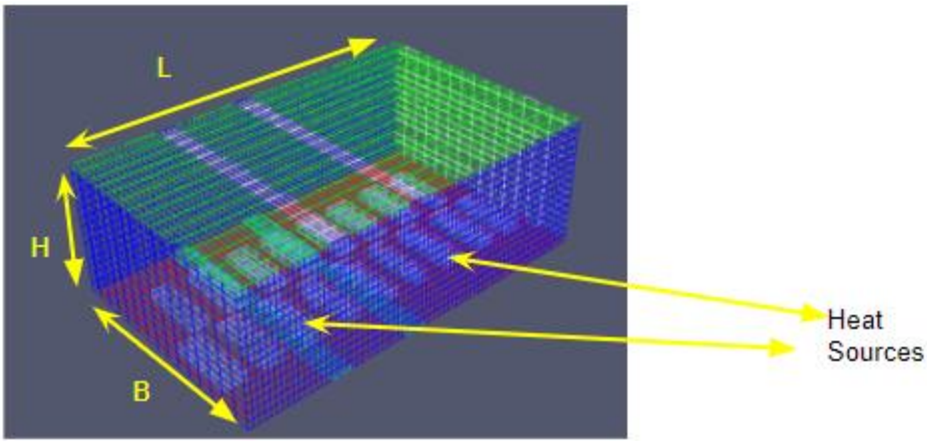

Figure 2 - Grid and Heat Sources

Here, *L = 180 mm, B = 112.5 mm, H = 62.7 mm*

The inlets have *length = 10 mm*, and *width = B* (runs across the breadth of the cuboid)

Heat sources have dimensions *30mm x 10 mm x 3 mm* and are 17 in number, spread along the channel's base. Heat sources are created by specifying zones on the bottom wall using topoSet. fvOptions is used to provide thermal conditions to these sources.

Both geometry and mesh were created using the blockMesh utility of OpenFOAM. Minimum cell size in the geometry is *~2.5 mm*. All cells have uniform gradations in all three directions.

4.2 Initial and Boundary Conditions

	Velocity	Pressure	Thermal
Inlet	*0.1 m/s*, fixed value	zeroGradient	*308 K*, fixed value
Outlet	zeroGradient	*0 Pa*, fixed value	zeroGradient
Heat Sources	noSlip	zeroGradient	Constant heat flux, *10000* W/m^3
Walls	noSlip	zeroGradient	zeroGradient

Walls – following patches fall under the category wall: floor_adb, ceiling, freeWalls, face_heated

Reference temperature *Tref = 300 K*

4.3 Solver

buoyantPimpleFoam solver is used to observing the transient variation of temperature due to turbulent flow of air through the channel. The simulation time step is set to ensure the Courant number stays less than 1.

The turbulence is modeled using the k-epsilon RAS model. Since forced convection is being considered, density is kept constant, and gravity is not taken into account (g = 0). The rest of the properties are listed below:

Molecular weight of air = 28.9 g/mol

Density = 1.225 kg/m^3

C_P *of air = 1006.43 kJ/kg.K*

Viscosity = 1.7894e-05 kg/m.s

Prandtl Number = 0.744176

The simulation is run for 90 seconds. Following commands are used in OpenFOAM v7 to run the simulation, in order: *blockMesh, topoSet, buoyantPimpleFoam*

3 case files have been generated, actual, grid independence study, and parameterized case.

5. Results and Discussions

5.1 Actual Case

Velocity:

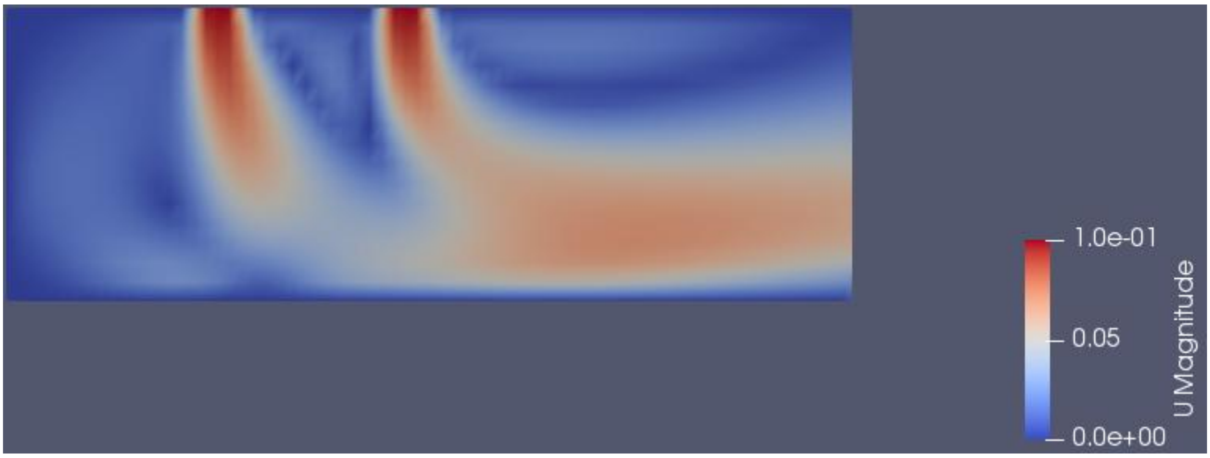

Figure 3 - Velocity Contours at Cross Section (z-normal, midplane)

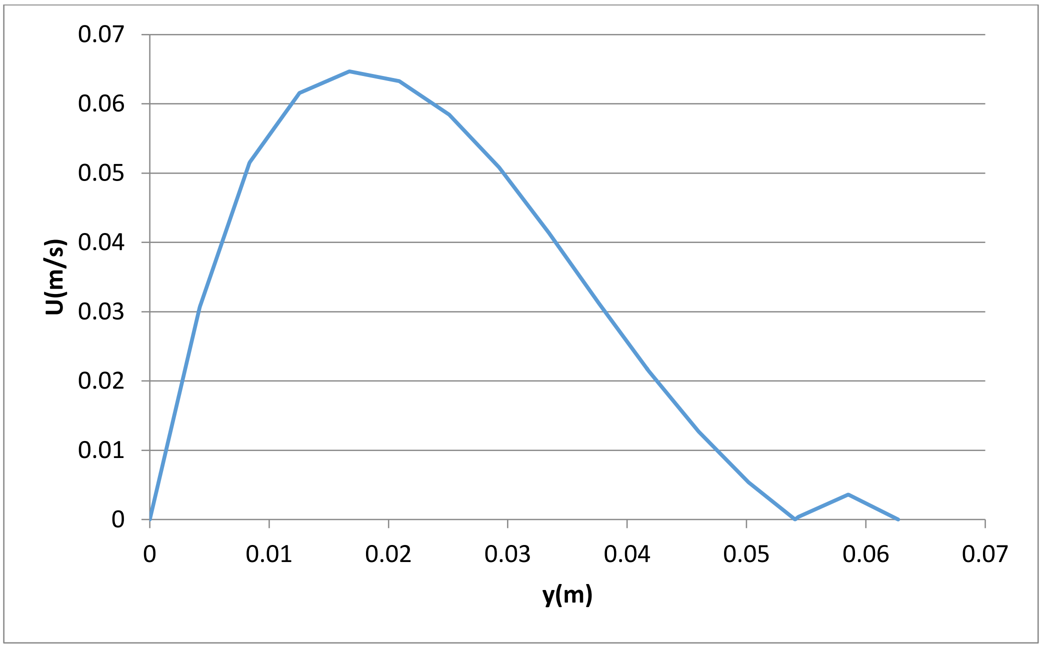

Figure 4 - Velocity Profile in y-direction, 10 mm before Outlet

Here we can see air enters from the top, and the peak velocity is attained closer to the bottom wall, and a stagnation region (in contours) is visible close to the wall opposite the Outlet.

This stagnation happens as all the flow is driven towards Outlet as there is no backpressure available.

The velocity is 0 only at the ends. The minima between 0 mm and 62.7 mm is tending to 0, not exactly 0.

Temperature (Note: in all cases, maximum temperature of the observed region is plotted):

Temperature is measured 1 mm above the heat source. This is the position where a thermistor would be placed in the physical model. It is plotted with respect to time. The following figure shows the location of cells considered while measuring temperature:

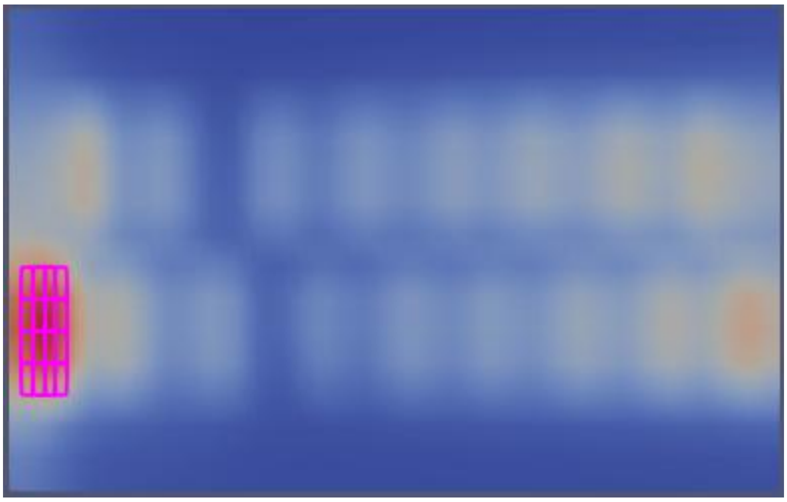

Figure 5 - Location of cells under observation

The cells under observation are chosen from the hottest region (close to the wall opposite the Outlet). Since this is the hottest region, the entire design of system will boil down to its temperature.

Figure 6 - Cross section (z-normal, mid-plane) temperature gradient inside geometry

The red regions in the above figure are the hottest; as we move from red to blue regions, the temperature decreases. This red region is located directly opposite Outlet.

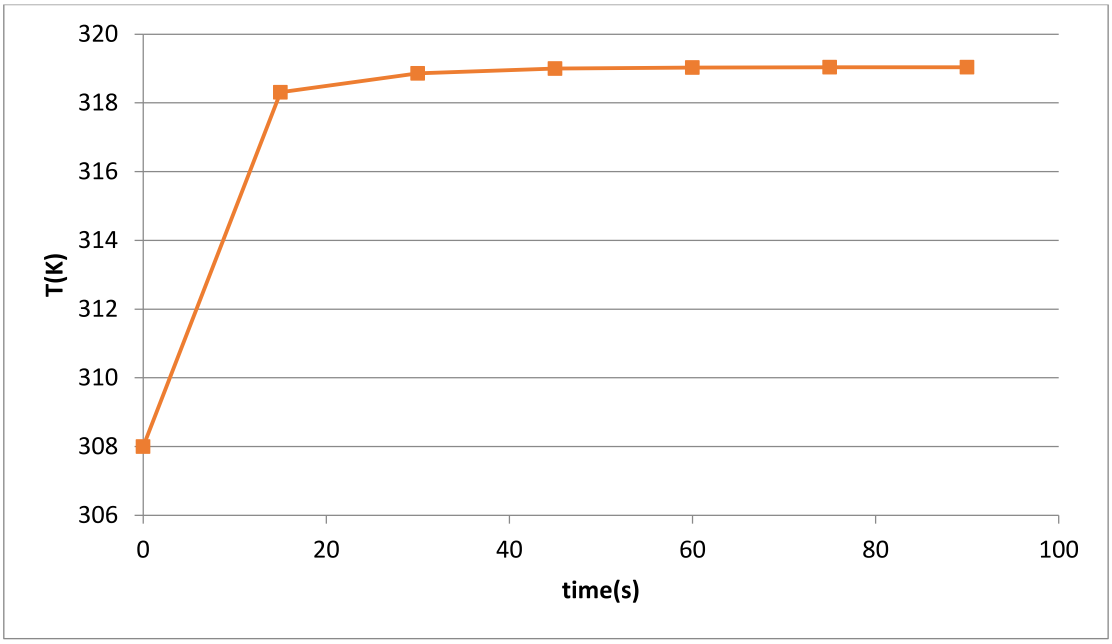

Figure 7 - Temperature variation of observed region with time

The temperature of the hottest region increases steadily, the rate decreases over time and finally attains equilibrium. At equilibrium, the rate of heat generation becomes equal to the heat being taken away by air.

5.2 Grid Independence Study

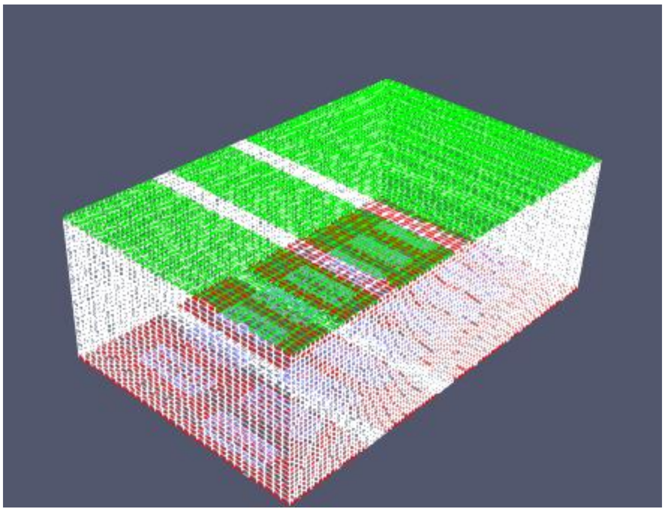

Figure 8 - Geometry with finer mesh

To study the dependence on grid size, a finer mesh of minimum element size ~2 mm was chosen. Mesh is still kept uniform throughout to match computational constraints.

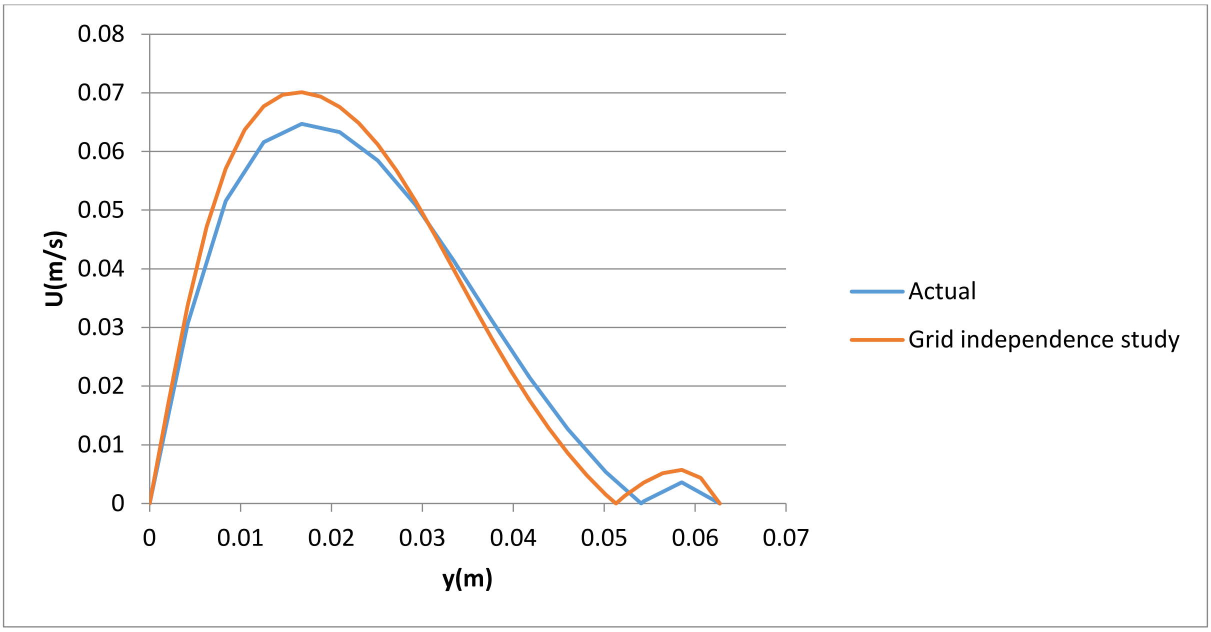

Figure 9 - Velocity Profile in y-direction, 10 mm before Outlet

Figure 10 - Cross section (z-normal, mid-plane) temperature gradient inside geometry

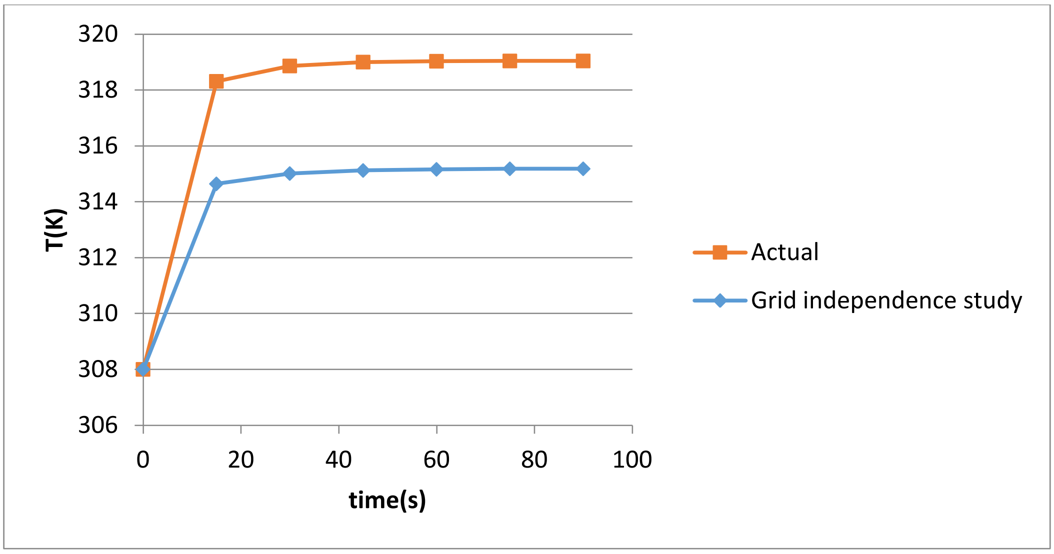

Figure 11 - Temperature variation of observed region with time

A variation in velocity and temperature is observed as the solver is able to calculate more precisely compared to the actual case. This is observed in the magnitudes of both velocity and temperature. However, the trend remains the same as the physics behind solving the problem hasn't changed.

5.3 Parametric Analysis

To see the effects of variation of parameters, the heat flux value was doubled (*20000 W/m³*). Velocity, mesh, and other parameters are kept the same as the initial case.

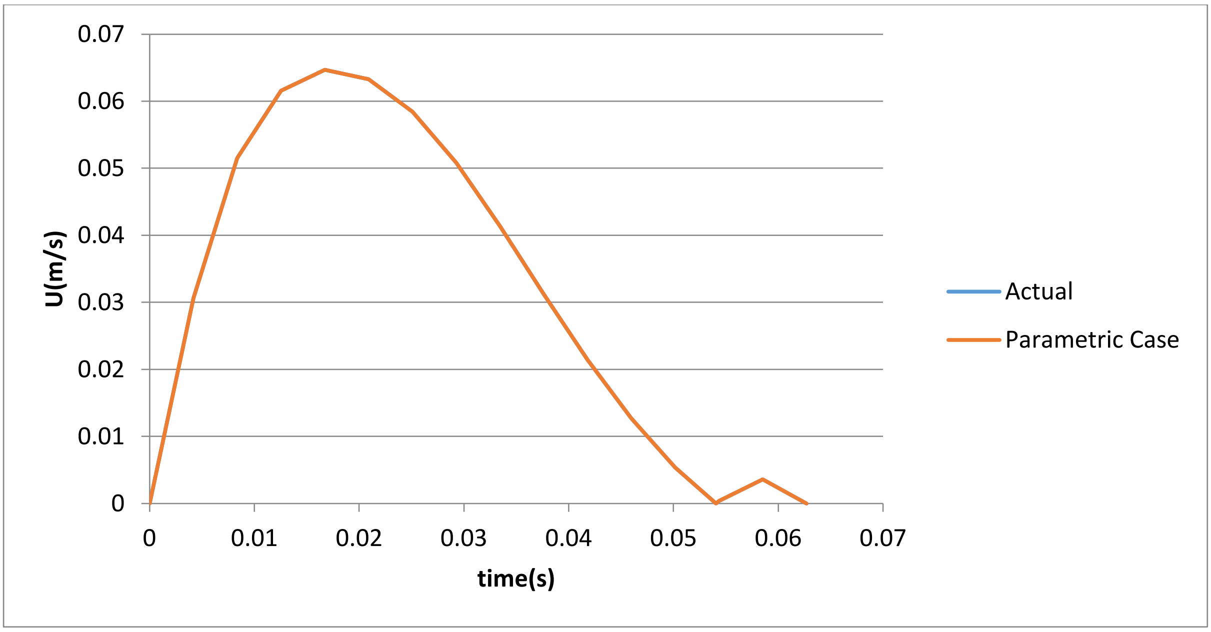

Figure 12 – Velocity Profile in y-direction, 10 mm before Outlet

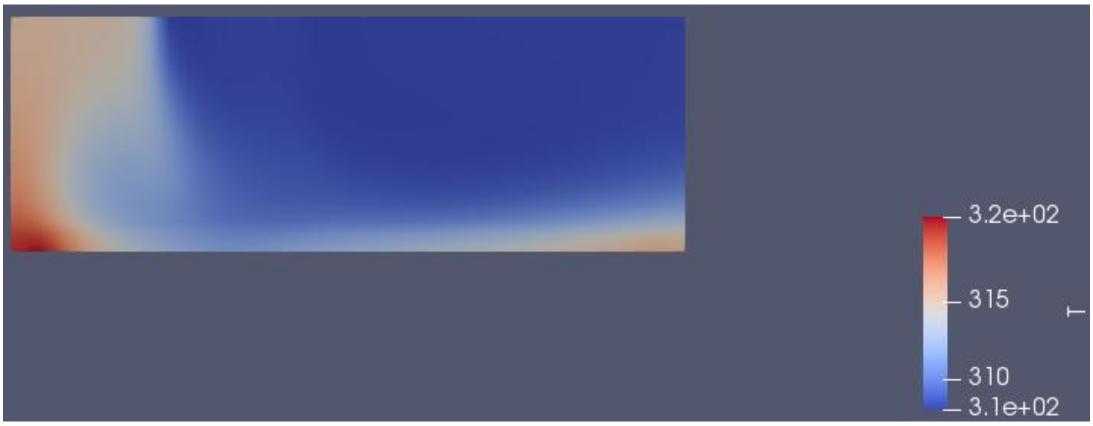

Figure 13 - Temperature profile of cross-section at the end of 90s

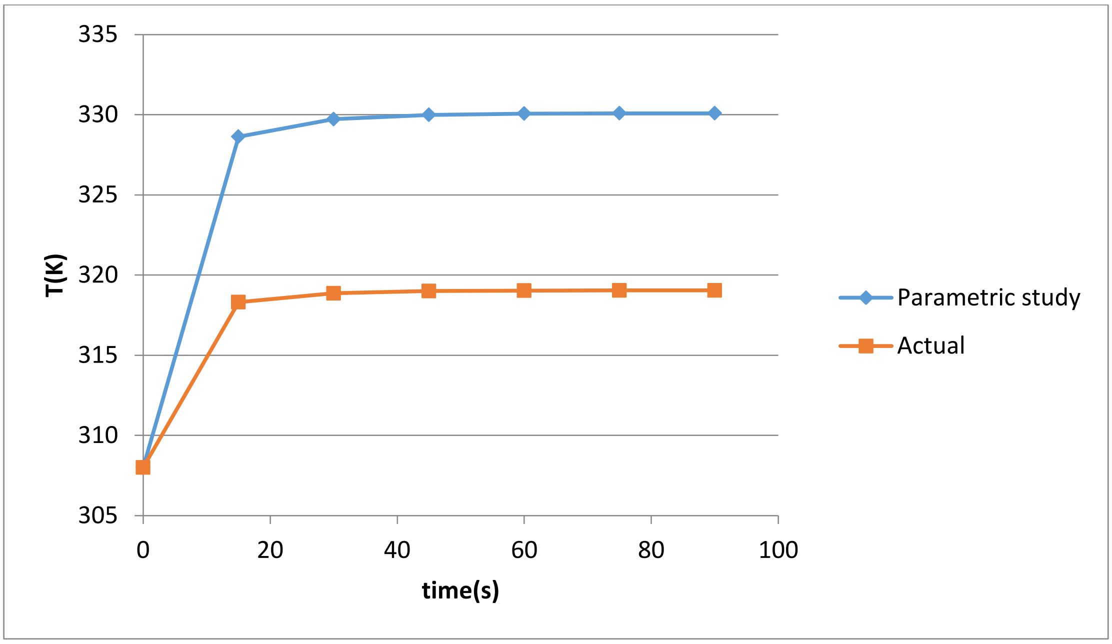

Figure 14 - Variation of temperature with time over the region of consideration

From the above figures, it can be observed that temperature increased in all regions. Trend is similar to the actual case since the temperature change is not large (~*11 K*), and equilibrium is achieved towards the end. Velocity remains exactly the same as the actual case since density differences due to temperature have been neglected during the simulation.

6. Conclusion

From the results, it can be seen that the system attains equilibrium with the flow of air. A maximum constant temperature is achieved by the end of the simulation. In the physical model, the temperature is expected to increase initially at a rate displayed by the results but later with a very low rate rather than being constant. This could be attributed to the absence of hindrances in the path of air and constant heat flux condition instead of a variable one.

Grid independence was not achieved since the regions where most of the phenomenon is happening have coarse mesh. Non-uniform refinement (more refined close to walls) needs to be made to get proper results independent of the element size.

7. Future Scope

This problem can be extended to the inclusion of cell body which could be cooled using conduction methods. The source heat flux could be varied with time, eventually cutting it off to observe cooling performance post heating run. To make it mimic a more realistic scenario, some obstructions could be introduced in the flow path, such as wires modeled as cylindrical recirculation zones. Overall the simulation could be run for a longer time leveling it with the real-time performance expected from the battery pack.

References

- Zul Hilmi Che Daud. Contribution to thermal behaviour study of lithium-ion battery for electric and hybrid electric vehicle. Mechanics [physics.med-ph]. Université de Bourgogne, 2014. English. ffNNT : 2014DIJOS078ff. fftel-01251555f
- Openfoam. OpenCFD Ltd, http://www.openfoam.org